Earth and Planetary Science Letters 439 (2016) 117–128

Contents lists available at ScienceDirect

Earth and Planetary Science Letters

www.elsevier.com/locate/epsl

Melting processes and mantle sources of lavas on Mercury

Olivier Namur [a,*], Max Collinet [b], Bernard Charlier [a,c], Timothy L. Grove [b], Francois Holtz [a], Catherine McCammon [d]

[a] Institut für Mineralogie, Leibniz Universität Hannover, 30167 Hannover, Germany
[b] Massachusetts Institute of Technology, Department of Earth, Atmospheric, and Planetary Sciences, Cambridge, MA 02139, USA
[c] Department of Geology, University of Liège, 4000 Sart Tilman, Belgium
[d] Bayerisches Geoinstitut, University of Bayreuth, 95440 Bayreuth, Germany

ARTICLE INFO

Article history:
Received 10 August 2015
Received in revised form 12 November 2015
Accepted 24 January 2016
Available online 8 February 2016
Editor: C. Sotin

Keywords:
MESSENGER
volcanism
phase equilibria
equilibrium melting
sulfur

ABSTRACT

The MESSENGER spacecraft provided geochemical data for surface rocks on Mercury. In this study, we use the major element composition of these lavas to constrain melting conditions and residual mantle sources on Mercury. We combine modelling and high-temperature (1320–1580 °C), low- to high-pressure (0.1 to 3 GPa) experiments on average compositions for the Northern Volcanic Plains (NVP) and the high-Mg region of the Intercrater Plains and Heavily Cratered Terrains (High-Mg IcP-HCT). Near-liquidus phase relations show that the S-free NVP and High-Mg IcP-HCT compositions are multiply saturated with forsterite and enstatite at 1450 °C – 1.3 GPa and 1570 °C – 1.7 GPa, respectively. For S-saturated melts (1.5–3 wt.% S), the multiple saturation point (MSP) is shifted to 1380 °C – 0.75 GPa for NVP and 1480 °C – 0.8 GPa for High-Mg IcP-HCT. To expand our experimental results to the range of surface compositions, we used and calibrated the pMELTS thermodynamic calculator and estimated phase equilibria of ~5800 compositions from the Mercurian surface and determined the P–T conditions of liquid–forsterite–enstatite MSP (1300–1600 °C; 0.25–1.25 GPa). Surface basalts were produced by 10 to 50% partial melting of variably enriched lherzolitic mantle sources. The relatively low pressure of the olivine–enstatite–liquid MSP seems most consistent with decompression batch melting and melts being segregated from their residues near the base of Mercury's ancient lithosphere. The average melting degree is lower for the young NVP (0.27 ± 0.04) than for the older IcP-HCT (0.46 ± 0.02), indicating that melt productivity decreased with time. The mantle potential temperature required to form Mercurian lavas and the initial depth of melting also decreased from the older High-Mg IcP-HCT terrane (1650 °C and 360 km) to the younger lavas covering the NVP regions (1410 °C and 160 km). This evolution supports strong secular cooling of Mercury's mantle between 4.2 and 3.7 Ga and explains why very little magmatic activity occurred after 3.7 Ga.

1. Introduction

One of the major findings based on data from the MESSENGER spacecraft is that volcanism at the surface of Mercury was widespread (Head et al., 2011; Denevi et al., 2013; Marchi et al., 2013; Thomas et al., 2014). The MESSENGER imagery revealed that surface volcanism produced kilometer-thick deposits (Head et al., 2011; Klimczak et al., 2012; Byrne et al., 2013). Based on the density of craters across the planet, it has been estimated that the whole surface of Mercury was resurfaced by volcanic activity and that the secondary volcanic crust was formed between 4.2 and 3.7 Ga (Weider et al., 2012; Marchi et al., 2013). A large portion of the planet (~27%) is dominated by crater-poor plains, with the largest occupying ~6% of the planet surface (Northern Volcanic Plains).

The compositions of primitive melts provide the principal evidence for interpreting the conditions of magma generation for which little information currently exists. The major element composition of the lavas of Mercury can be used to decode mantle melting processes and mantle sources. These lavas may have been produced by remelting of cumulates of a solidified magma ocean (Brown and Elkins-Tanton, 2009; Charlier et al., 2013; Vander Kaaden and McCubbin, 2016) or may represent melts of an undifferentiated primordial mantle source region (Zolotov et al., 2013; Malavergne et al., 2014). The observed melts of the Mercurian mantle provide a record of the large-scale differentiation of the planet and the formation of the ~35 km thick magmatic crust (Padovan et al., 2015). Although the bulk composition of the Mer-

* Corresponding author.
E-mail address: o.namur@mineralogie.uni-hannover.de (O. Namur).

http://dx.doi.org/10.1016/j.epsl.2016.01.030
0012-821X/

curian mantle is poorly constrained, it has been suggested that it may be similar to the silicate fraction of metal-rich chondritic material (enstatite chondrite (EH) and/or bencubbinite (CB); Taylor and Scott, 2003; Malavergne et al., 2010).

In this study, experiments and modelling are used to link the composition of the volcanic secondary crust with the mantle source materials. We used chemical information from MESSENGER (Weider et al., 2012, 2015; Peplowski et al., 2015) to calculate two average compositions representative of the High-Mg regions and the Northern Volcanic Plains. Based on high-pressure, high-temperature experiments, we discuss phase equilibria of Mercurian basalts and, in particular, we identified forsterite–enstatite–liquid multiple saturation points (MSP) that we interpret as the conditions of mantle-melt equilibration prior to eruption (Asimow and Longhi, 2004). We also discuss the role of sulfur on phase equilibria of Mercurian mantle melts. Using thermodynamic modelling with the MELTS/pMELTS algorithms, we calculated high-temperature phase equilibria of ~5800 compositions from Mercury's crust (Weider et al., 2015), corrected them empirically for the effect of sulfur, and used these data to infer the present-day mineralogy of the Mercurian mantle as well as the range of pressure and temperature conditions for melting. We also discuss the thermal evolution of the Mercurian mantle between 4.2 and 3.7 Ga and suggest that surface lavas were produced by melting material of variably enriched lherzolitic sources.

2. Compositional variability at the surface of Mercury

The surface of Mercury is Mg-rich and Al-, Ca- and Fe-poor compared to terrestrial and lunar crustal material (Weider et al., 2015). It is assumed to be dominated by Mg-rich silicate minerals (forsterite, enstatite), plagioclase, sulfides [(Ca, Mg, Fe)S] and possibly minor Fe-silicides (Weider et al., 2012, 2014).

Based on XRS measurements acquired during solar flares from April to December 2011, two main geochemical provinces were discriminated (Weider et al., 2012; Fig. 1): (1) the Northern Volcanic Plains (NVP) with low Mg/Si ratios, Ca/Si ratios and S/Si ratios and high Al/Si ratios; (2) the Intercrater Plains and Heavily Cratered Terrains (IcP-HCT) with, on average, higher Mg/Si ratios, Ca/Si ratios and S/Si ratios and lower Al/Si ratios. Based on analyses with better spatial resolutions (April 2011 to December 2013), the geochemical subdivision of Mercury's surface has been refined (Fig. 1). The NVP is subdivided into two regions: the low-Mg NVP at latitudes higher than 60°N and the high-Mg NVP (~30°W–100°E; ~30°–60°N). The IcP-HCT is more complicated and can broadly be subdivided into a high-Mg region, which may contain an internal high-Mg and high-Ca region and a rather heterogeneous intermediate region. K and Na are low in IcP-HCT ($K < 1000$ ppm; Na/Si: 0.10 ± 0.01) and high in high-Mg NVP ($K > 1200$ ppm and Na/Si: 0.12 ± 0.02) and even higher in low-Mg NVP ($K > 1500$ ppm; Na/Si: 0.19 ± 0.03; Peplowski et al., 2012, 2014). Mercury's surface also shows several Smooth Plains (SP) including the Caloris basin, the Rachmaninoff basin, and the high-Al Smooth Plain. Sulfur is generally higher in regions with high Mg/Si and Ca/Si ratios (IcP-HCT) and lower in NVP (Weider et al., 2015). As shown in Fig. 1, the different geochemical terranes cannot be related to each other by a process of fractionation or accumulation of common minerals such as forsterite and enstatite, suggesting that lavas at the surface of the planet may represent primary mantle-derived melts (Fig. 1).

For this study, we recalculated surface compositions (Fig. 2 and Fig. S1) using the most recent maps produced from MESSENGER XRS data (Weider et al., 2015). We focused on the northern hemisphere for which the spatial resolution of MESSENGER measurements is the highest. We combined individual maps of Mg/Si, Ca/Si, Al/Si and S/Si and only worked on pixels for which those 4 ratios

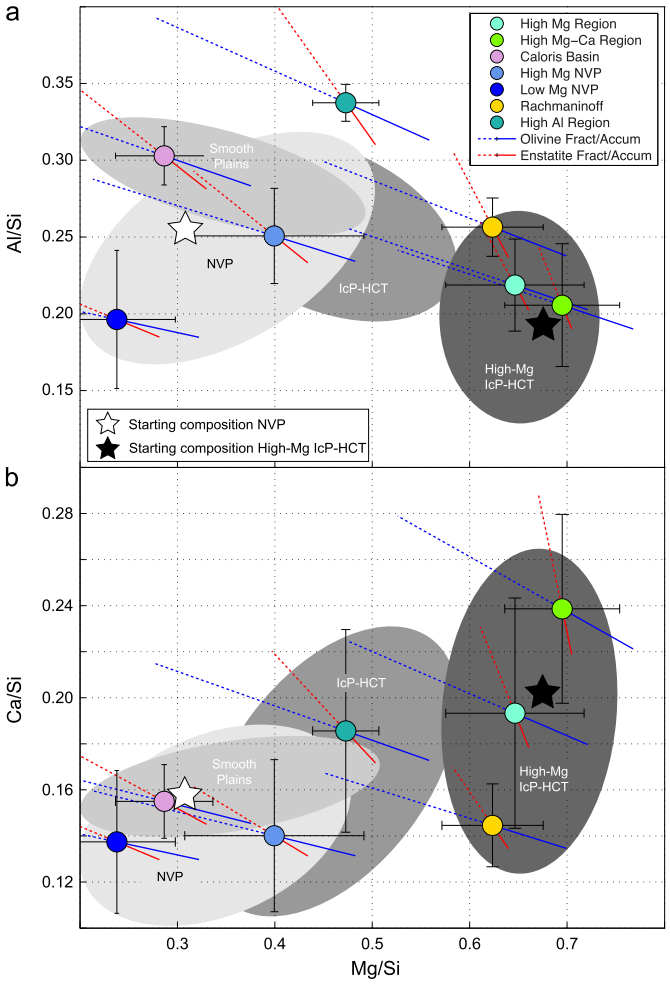

Fig. 1. Elemental weight ratios inferred from MESSENGER XRS data. (a) Al/Si versus Mg/Si. (b) Ca/Si versus Mg/Si. Colored circles show average compositions of the geochemical terranes identified by Weider et al. (2015). The 1σ error bars are shown for each terrane. Lines radiating from each symbol show the compositional effect of accumulating (plain line) forsterite (blue) or enstatite (red) or fractionating (dashed line) olivine or enstatite. The different geochemical provinces cannot be linked to each other by these lines, indicating that their average compositions cannot be related by any process of accumulation and/or fractional crystallization. Compositional fields in grey-scale show the range of compositions of lavas from the Northern Volcanic Plains (NVP), the Smooth Plains (SP), the Intercrater Plains and Heavily Cratered Terrains (IcP-HCT) and the High-Mg IcP-HCT region inferred from pixel analyses (1.25° × 1.25° pixel groups) of the elemental maps of Weider et al. (2015). Black and white stars represent the starting compositions used in experiments. (For interpretation of the references to color in this figure legend, the reader is referred to the web version of this article.)

were measured. This method allows investigating only some parts of the northern hemisphere because the Ca/Si map is not complete. We produced >5800 groups of 25 pixels (1.25° latitude × 1.25° longitude) that we converted to volatile-free chemical compositions (SiO_2, Al_2O_3, MgO and CaO; Fig. 2). Each pixel group was assigned to the geochemical terrane in which it is located (NVP, including the low-Mg and high-Mg NVP; IcP-HCT, excluding the high-Mg region; high-Mg region of the IcP-HCT; SP, including Caloris basin and Rachmaninoff basin) to which we attributed specific concentrations for minor elements (Nittler et al., 2011; Peplowski et al., 2015). For Na_2O, we considered that NVP lavas have high Na_2O contents (Na/Si: 0.20; ~7 wt.% Na_2O), SP lavas have intermediate Na_2O contents (Na/Si: 0.14; ~5 wt.% Na_2O) and IcP-HCT lavas have lower Na_2O contents (Na/Si: 0.06; ~2 wt.% Na_2O; Peplowski et al., 2014). Large chemical variability is observed in calculated compositions and the lavas from different geochemical terranes significantly overlap (Fig. 2).